Research Square

Preprints are preliminary reports that have not undergone peer review.
They should not be considered conclusive, used to inform clinical practice,
or referenced by the media as validated information.

Upregulation of EZH2 and E2F1 in combination with NF2 alterations underlies the molecular characteristics of aggressive meningiomas

Ryota Sasao
Saiseikai Yokohamashi Tobu Hospital
Tetsuya Takimoto
Fujita Health University
Kohei Nakamura
Keio University School of Medicine
Kiyotaka Yokogami
Miyazaki University School of Medicine
Shinji Yamashita
Miyazaki University School of Medicine
Eriko Aimono
LUMIPATH clinic
Shigeo Ohba
Fujita Health University School of Medicine
Hiroshi Nishihara
Keio University School of Medicine
Hideyuki Saya
Fujita Health University
Hikaru Sasaki
sasaki-hikaru-ki@ihwg.jp

Keio University School of Medicine

Research Article

Keywords: meningioma, E2F, EZH2, EZH2 inhibitor, NF2, tazemetostat

Posted Date: June 1st, 2026

DOI: https://doi.org/10.21203/rs.3.rs-9722243/v1

License: This work is licensed under a Creative Commons Attribution 4.0 International License.
Read Full License

Additional Declarations: No competing interests reported.

Abstract

Coding variations do not significantly contribute to tumor aggressiveness in meningiomas except for rare alterations in *CDKN2A* and *TERT*. The aim of this study was to investigate specific molecular pathways as potential therapeutic targets.

A discovery cohort of 35 meningiomas, including 26 high-grade tumors, was investigated for genetic alterations and gene expression profiling, and analyzed by unsupervised hierarchical clustering, gene set enrichment analysis (GSEA) and gene set variation analysis (GSVA). The results were validated by OncoPrint analyses in a larger dataset published previously. The efficacy of an EZH2 inhibitor was evaluated in multiple meningioma cell lines.

Tumors in the discovery cohort were classified into three clusters (Cluster M: Low, Mid, High) using hierarchical clustering based on genes differentially expressed across CNS WHO grades. These clusters correlated with overall survival and WHO grade. GSEA between the subgroups of Cluster M demonstrated that meningiomas gain aggressiveness through the downregulation of gene sets associated with the immune response (Low→Mid), and subsequently by the upregulation of those associated with cell cycle and cell proliferation (Mid→High). These results were corroborated by GSVA based on the enrichment score of the Hallmark gene sets as well as hierarchical clustering based on copy number losses, with enrichment of the E2F target and MYC target gene sets in high-grade clusters. OncoPrint analyses in the published dataset showed that the most aggressive type of meningiomas is characterized by upregulation of EZH2 as well as E2F1, but not MYC, in combination with *NF2* alterations. Meningioma cell growth was suppressed by an EZH2 inhibitor with possible correlation with EZH2 expression.

Meningiomas with *NF2* alterations exhibit distinct biological behaviors depending on the expression of EZH2 and E2F1, and aggressive meningiomas are characterized by the upregulation of these pathways in combination with *NF2* alterations. EZH2 is a pivotal therapeutic target for high-grade meningiomas.

Introduction

Meningiomas account for over 35% of all primary central nervous system tumors. Approximately 20% of meningiomas are WHO grade 2 (atypical) or grade 3 (anaplastic) [19]. Most of these higher-grade meningiomas are refractory to repeated surgery and radiotherapy, and are ultimately fatal, as there is currently no established medical therapy for them.

Recent advances in the molecular characterization of meningiomas have been remarkable, and several driver gene mutations have been reported; more than half of meningiomas are associated with mutations in the *NF2* gene and/or monosomy of chromosome 22, and the rest are associated with mutations in genes such as *AKT1*, *SMO*, *KLF4*, or *TRAF7* [30]. These driver gene mutations are mutually exclusive and are significantly associated with tumor location, histological subtype, and histological grading. Moreover, molecular-based stratification of meningiomas was shown to be more closely

associated with recurrence-free survival than WHO grading [24, 29]. Nassiri et al. proposed four molecular groups of meningioma based on the integrative analysis of multiple datasets: immunogenic (MG1), benign *NF2* wild-type (MG2), hypermetabolic (MG3), and proliferative (MG4), with the most unfavorable outcomes for MG4 tumors. However, these molecular-based classifications have not led to effective personalized treatment so far.

Most higher-grade meningiomas have been shown to be associated with multiple chromosomal number aberrations (CNAs) in addition to *NF2* mutations; however, medical therapies targeting the NF2 pathway have failed to demonstrate an objective response for treatment-refractory meningiomas [3, 31]. Indeed, unlike in gliomas, subsequent driver gene mutations responsible for the malignant progression of *NF2*-mutated meningiomas have rarely been reported in the literature, with the exception of homozygous deletions in the *Cyclin-Dependent Kinase Inhibitor 2A* (*CDKN2A*) gene and mutations in the promoter region of the *Telomerase Reverse Transcriptase* (*TERT*) gene. Thus, a specific expression profile rather than a driver gene mutation might guide a rational therapeutic approach for treatment-refractory meningiomas. The aim of this study was to stratify meningiomas primarily based on their expression profiles, and to find a key pathway that could be a therapeutic target. Immunohistochemistry was also performed for candidate target molecules for currently available therapies to determine if there was any correlation with tumor malignancy.

Materials and Methods

Patients

We reviewed the frozen brain tumor tissue bank at the Department of Neurosurgery, Keio University Hospital, and identified 26 tumors resected from 1998 to 2020 with a diagnosis of grade II or III meningioma based on institutional histopathological records. These included 22 atypical meningiomas (WHO grade II) and 4 anaplastic meningiomas (WHO grade III). Of these, tissue from 12 of the 22 atypical meningiomas and all 4 anaplastic meningiomas was obtained during surgery for tumor recurrence; four of these were recurrences after radiotherapy and the others after observation. For comparison, nine grade I meningiomas that were completely resected at the initial surgery and had shown no evidence of recurrence for at least 8 years were also included. Histopathological diagnosis and malignancy grade of the tumors were confirmed by the pathologist (HN) based on the 2016 WHO criteria [17]. Tumor grade was subsequently updated as per the 2021 criteria based on the results of next generation sequencing (NGS)[2]. Clinical information was obtained from the medical record of each patient and updated as of August 2025. For survival analysis, overall survival was calculated from the date of initial surgery.

DNA and RNA extraction

PAXgene-fixed, paraffin-embedded (PFPE) samples were prepared from frozen tumor tissues using the PAXgene Tissue System (Qiagen, the Netherlands). DNA and RNA were extracted using the Maxwell RSC Instrument (Promega, WI) according to the manufacturer's protocol. The quality of DNA and RNA was assessed based on a threshold of DNA integrity number (DIN) ≥ 2.0, RNA integrity number (RIN) ≥ 2.0, and DV300 ≥ 30.

Cancer genome profiling

Genomic DNA was analyzed for somatic mutations and copy number alterations using the PleSSion-Rapid-Neo platform comprising 164 cancer genes as previously described [23, 25] (Supplementary Table S1).

Expression profiling using nCounter system

mRNA expression was analyzed in 35 cases using the nCounter PanCancer Pathways Panel, comprising 770 genes from 13 canonical pathways (NanoString Technologies, WA). Total RNA was hybridized with preset probes and evaluated using the NanoString nCounter digital analyzer. Data were analyzed using nSolver analysis software (NanoString Technologies, WA), and the mRNA profiling data were normalized using housekeeping genes. Normalized data were log2-transformed for further analysis.

Unsupervised hierarchical clustering, differentially expressed genes

To generate the dendrogram, hierarchical clustering was performed using expression data from the nCounter analysis. Euclidean distances were calculated using the dist function from the stats package in R version 4.3.1 [34], with expression values scaled to Z-scores for each gene. Clusters were identified using the complete linkage method via the hclust function in the same package, based on the Euclidean distance. Differentially expressed genes (DEGs) among the three histological grades were identified using ANOVA. The correlation coefficients between each differentially expressed gene and histological grade were calculated. Genes with correlation coefficients greater than 0.5 were classified as positively correlated, whereas those with coefficients less than − 0.5 were classified as negatively correlated.

GSEA, GSVA, hierarchical clustering based on copy number loss

Gene set enrichment analysis (GSEA) was performed using the fgsea package with fold changes in gene expression between samples from each pair of clusters [12, 21, 32]. The GO Biological Process, KEGG Pathway, and Hallmark gene sets from MSigDB were included in the analysis [14]. A volcano plot was generated using the normalized enrichment scores and adjusted p-values from GSEA with the EnhancedVolcano package [1]. Additionally, gene set variation analysis (GSVA) was conducted to score representative functions using the Hallmark gene sets in each sample based on gene expression values

[9, 13]. A volcano plot was generated based on the fold change and false discovery rate (FDR) calculated using fold change, the Wilcoxon rank-sum test, and adjusted p-values from GSVA with the EnhancedVolcano package [1]. Unsupervised hierarchical clustering based on the detected copy number losses was also performed.

Cell lines, cell cycle, and viability analyses

Three malignant meningioma cell lines (IOMM-Lee, HKM-MM, MZ857MM) were used and cultured as previously described [38]. Cell cycle analyses were performed as previously described [38]. For apoptosis analysis (annexin V assay), the MEBCYTO® Apoptosis Kit (MBL, Nagoya, Japan) was used. A histogram of the cell cycle distribution was generated from 5,000 events per sample, and data were analyzed using Guava® Cell Cycle and Guava® ExpressPlusBlue software, respectively. Tazemetostat was purchased from Selleck (Tokyo, Japan). In the water-soluble tetrazolium salt (WST-8) assay, the culture medium was removed and replaced with various concentrations of tazemetostat-containing medium. After the indicated incubation periods, 20 µl WST-8 dye (Cell Counting Kit-8; Dojindo Corporation, Kumamoto, Japan) was added to each well. After 3 hours, the plates were read at 450 nm/655 nm. Statistical evaluations were performed using Student's t-test.

Immunofluorescence

Meningioma cells were seeded at a density of 1×10^4 cells per well on Matsunami glass coverslips in 24-well plates. The procedures were described in a previous report (19). Cells were mounted in a DAPI-containing mounting medium and then photographed using an all-in-one fluorescence microscope (Keyence model BZ-X800L, Osaka, Japan). The primary antibodies were vimentin (M0725, 1:1 dilution) (Agilent Technology, Santa Clara, CA, USA), enhancer of zeste homolog 2 (EZH2) (#5246S, 1:100 dilution) and trimethylation of histone 3 lysine 27 (H3K27m3) (#9733S, 1:100 dilution) (CST Japan, Tokyo, Japan).

Western blotting

Western blotting was performed as previously described [37]. Quantification of immunoblotting band intensity was performed using iBright analysis software (Invitrogen), and values were normalized to β-actin bands. The primary antibodies were EZH2 (#5246S, 1:1000 dilution) and beta-actin (A5441, 1:5000 dilution) (Sigma-Aldrich, Tokyo, Japan).

Immunohistochemistry

Because these molecules are targets of currently available therapies, the expression of somatostatin receptor subtype 2A (SSTR2A), platelet derived frowth factor receptors (PDGFRs), and AT-rich interaction domain 1A (ARID1A) was examined in PFPE sections by immunohistochemistry using an anti-SSTR-2 antibody (UMB1, Abcam, UK), anti-PDGFR alpha and beta antibodies (Y92, Abcam, UK), and an anti-ARID1A antibody (EPR13501, Abcam, UK). All slides were scanned at 20× magnification to produce high-

resolution digital images of the tissue using a scanner (NanoZoomer S210, Hamamatsu Photonics K.K.). The images were visualized using a software program, NanoZoomer Digital Pathology (NDP.view2 U12388-01, Hamamatsu Photonics K.K., Hamamatsu City, Japan). In the images, individual cells and their subcellular compartments (i.e., nucleus, cytoplasm, and cell membrane) were first identified. Cells were then classified as either positive or negative based on the relative expression of the biomarker of interest in one or more subcellular compartments. The positive cells were further classified as having strong (3+), moderate (2+), or weak (1+) staining based on the biomarker signal intensity. The H-score, a reliable metric, was calculated as follows: (1× percentage of weak staining) + (2× percentage of moderate staining) + (3× percentage of strong staining) within the target region, ranging from 0 to 300 [20].

Results

Cancer genome profiling and reappraisal of tumor grading

Next-generation sequencing using the PleSSion-Rapid-Neo platform was performed on 35 tumors. Detailed results are shown in Supplementary Table S2. Pathogenic mutations were reported in 23 cases. The most commonly affected genes included *NF2* (mutated in 20 cases), *CDKN2A* (homozygous deletion in 3 cases), and *TERT* (promoter mutations in 2 cases). Accordingly, the grade of five grade II tumors was changed to grade 3 based on the 2021 WHO classification, and ultimately, 9 grade 1 (without recurrence for more than 8 years), 17 grade 2, and 9 grade 3 meningiomas were included in the subsequent analyses.

Clustering based on differentially expressed genes across histological grade

Unsupervised clustering based on the mRNA expression of 770 genes in the nCounter PanCancer Pathways Panel is shown in Supplementary Fig S1. Notably, the seven oldest samples were segregated into a single cluster (cases 1–7), likely due to RNA degradation from long-term storage. Therefore, these seven cases were excluded from further analyses. In the unsupervised clustering of the remaining 28 cases, however, grade 1 tumors were dispersed, and the clustering did not appear to reflect clinical characteristics well (Supplementary Fig S2). Thus, we next focused on DEGs across tumor grades, because WHO tumor grading generally correlates well with the biological behavior of meningiomas.

Based on ANOVA testing across tumor grades for the 28 cases, 39 positively correlated and 20 negatively correlated DEGs were identified (Supplementary Table S3). Hierarchical clustering based on these DEGs divided the cases into three clusters (Fig. 1A); one consisted of eight grade 1 and three grade 2 tumors, the second consisted of one grade 1, five grade 2, and two grade 3 tumors, and the third consisted of four grade 2 and five grade 3 tumors. This grouping appeared to correlate more closely with the histological grade of meningiomas than the clustering based on 770 genes, and correlated well with

patient overall survival (Supplementary Fig S3). The resulting 3 groups were named Low, Mid, and High, and this newly created cluster was defined as Cluster M (Fig. 1B).

Differentially expressed genes between three meningioma groups

We explored DEGs and gene sets between each pair of groups within Cluster M (Supplementary Tables S4 and S5). GSEA revealed a predominant downregulation of specific gene sets in the Mid group compared to the Low group, and a predominant upregulation in the High group compared to the Mid group; gene sets associated with vascular system development and immune regulation were downregulated in the Mid group compared to the Low group, and those associated with DNA replication and the cell cycle were upregulated in the High group compared to the Mid group. (Fig. 2, Supplementary Tables S6 and S7). In both the Mid vs. Low and High vs. Mid comparisons, the E2F transcription factor (E2F) target gene set was enriched in the more malignant group of Cluster M.

Hierarchical clustering based on molecular pathway

GSVA was performed using the Hallmark gene sets, and each sample was assigned an enrichment score for each of the gene sets. Hierarchical clustering based on the enrichment score divided the samples into two clusters; one comprised all Low tumors, half of the Mid tumors, and one High tumor; the other comprised all but one of the High tumors, and the remaining half of the Mid tumors (Fig. 3A). Therefore, hierarchical clustering based on enrichment score correlated well with Cluster M as well as tumor histological grade. When comparing the two clusters, gene sets associated with cell proliferation and the cell cycle, including MYC Proto-Oncogene (MYC) targets v1 and E2F targets, were specifically upregulated, and those associated with the immune/inflammatory response and biological defense, including xenobiotic metabolism, complement, and IL6/JAK/STAT3 signaling, were downregulated in the cluster composed of High and Mid tumors compared to the cluster containing all grade 1 tumors (Fig. 3, Supplementary Table S8). Thus, hierarchical clustering based on enrichment score validated the results of GSEA in Cluster M, highlighting that upregulation of cell proliferation as well as downregulation of the immune/inflammatory response were among the most crucial changes in the malignant transformation of meningiomas.

Hierarchical clustering based on copy number loss

Hierarchical clustering based on copy number loss divided the tumors into two clusters; one was composed of six High and three Mid tumors, and the other was further separated into three sub-clusters, with the largest group composed of ten Low and five Mid tumors. Therefore, this clustering was also correlated with Cluster M as well as tumor histological grade (Supplementary Fig S4). In addition, the clustering was shown to be correlated with the enrichment score of MYC targets and E2F targets.

OncoPrint analyses of E2F1, EZH2, and MYC expression based on published data

The GSVA and GSEA results for Cluster M, which correlated with the pattern of copy number loss, demonstrated that aggressive meningiomas are characterized by the activation of pathways associated with cell proliferation, including E2F and MYC targets. To confirm the consistency of these results in a larger dataset, we performed OncoPrint analyses using a previously published dataset (https://www.cbioportal.org) [24]. The E2F1/NF2 OncoPrint demonstrated that tumors with high E2F1 expression in combination with *NF2* alterations were mostly MG4 (proliferative), while most of the MG1 (immunogenic) tumors were associated with low E2F1 expression (Fig. 4). Therefore, tumors with *NF2* alterations appeared biologically different depending on the degree of E2F1 expression. Next, we evaluated EZH2 expression using OncoPrint, because *EZH2* is among the target genes of E2F1 and the EZH2 inhibitor, tazemetostat, is FDA-approved. As expected, the EZH2 OncoPrint showed similar results; the tumors with high EZH2 expression in combination with *NF2* alterations were mostly MG4, while most of the MG1 tumors were associated with low EZH2 expression (Fig. 4). On the other hand, in the OncoPrint analysis with *NF2* and MYC, although most of the tumors with *NF2* alterations and high MYC expression were either MG4 or MG3, some MG1 tumors were also present within this group. Moreover, the MG1 tumors were rather dispersed regardless of the degree of MYC expression as compared with expression of E2F and EZH2 (Fig. 4).

Tazemetostat suppresses meningioma cell growth in an EZH2-dependent manner

Next, we investigated the efficacy of an EZH2 inhibitor on meningioma cell lines. Tazemetostat suppressed the growth of meningioma cell lines in a concentration- and time-dependent manner, with the strongest inhibitory effect observed in IOMM-Lee (Fig. 5A, Supplementary Fig S5). Cell cycle analysis showed that tazemetostat increased the sub-G1 population and induced apoptosis, especially in IOMM-Lee cells (Fig. 5B, C, Supplementary Figs S6 and S7). Western blot analysis showed strong expression of EZH2 in IOMM-Lee cells and weak expression in MZ857MM cells, suggesting that the efficacy of tazemetostat correlates with EZH2 expression (Fig. 5D, Supplementary Fig S8). In the immunofluorescence study, tazemetostat was shown to decrease trimethylation of H3K27, but not EZH2 (Fig. 5E, Supplementary Fig S9).

Immunohistochemistry

Immunohistochemistry for SSTR2A, PDGFRs, and ARID1A was performed in the 28 cases (9 grade 1, 12 grade 2, and 7 grade 3; or 11 Low, 8 Mid, and 9 High tumors as defined in Cluster M). Expression of ARID1A was increased in higher-grade as well as Mid/High meningiomas compared to grade 1 and Low tumors ($p = 0.05$ for Cluster M, $p = 0.006$ for histological grade) (Supplementary Figs S10 and S11). On

the other hand, expression of SSTR2A and PDGFRs was not associated with either tumor grade or Cluster M.

Discussion

Although molecular-based classifications were shown to successfully stratify meningiomas according to their biological aggressiveness [6, 24, 29], there is currently no established effective medical therapy. Previous reports suggested that most aggressive meningiomas are associated with mutations in the *NF2* gene in combination with chromosomal instability [7, 10]. However, except for *CDKN2A* homozygous deletion, *TERT* promoter mutations, and *SMARCB1* mutations in small subsets of patients, recurrent driver gene mutations occurring subsequent to *NF2* mutations have rarely been reported as potential therapeutic targets [10]. Indeed, Harmanci et al. reported that the driver gene mutations significantly associated with a diagnosis of atypical meningioma were only *NF2* and *SMARCB1* among 556 meningiomas, and suggested that coding variations do not significantly contribute to the risk of developing the atypical phenotype [10]. Given that therapies targeting *NF2* mutations have not been very promising so far, molecular therapy for aggressive meningiomas should probably target specific molecular pathways rather than gene mutations, unlike in many other cancers. Thus, we revisited expression profiling to elucidate key molecular characteristics of aggressive meningiomas.

The literature suggests that the aggressive phenotype of meningiomas is associated with the enrichment of cell-cycle regulation and proliferation-associated networks such as MYC, Forkhead Box M1 (FOXM1), and E2F, whereas less aggressive meningiomas are enriched for pathways involved in immune regulation and signaling [10, 24, 26]. In the present study, Cluster M, the meningioma grouping identified by hierarchical clustering based on DEGs between histological grades, appears to correlate with tumor aggressiveness. Both GSEA between the groups of Cluster M and hierarchical clustering based on Hallmark enrichment score showed that, in line with the literature, genes associated with the cell cycle and DNA replication were upregulated and those associated with immune/inflammatory response and vascular development were downregulated in aggressive meningiomas as compared with less aggressive tumors. Furthermore, the present study suggested that when comparing Low versus Mid and Mid versus High, the first step of malignant transformation in meningiomas might involve the downregulation of immune/inflammatory responses, while the second step might involve the upregulation of cell cycle-related genes (Fig. 2), suggesting that these malignant processes may be sequential. Moreover, the correlation between clustering based on copy number loss and the enrichment score of E2F/MYC targets and Cluster M suggested that the pattern of copy number loss was associated with the activation of pathways relevant to these oncogenes, and with tumor aggressiveness, corroborating recent recommendations for meningioma grading [28]. Taken together, two approaches, or a combination of these, should be considered as potential therapeutic approaches for high-grade meningiomas: restoration of the immune response and inhibition of cell proliferation.

Previous studies have shown that *E2F1* upregulation is among characteristic of high-grade meningiomas [10, 24, 36]. Importantly, through OncoPrint analyses of a large dataset, the present study demonstrated

that the most aggressive types of meningiomas, such as the MG4 group described by Nassiri et al., are characterized by a combination of increased expression of E2F1 and alterations in the *NF2* gene. Furthermore, tumors with *NF2* alterations were shown to be biologically distinct depending on the degree of E2F1 expression. Indeed, tumors with low E2F1 expression were shown to be either MG1 or MG2, even in the presence of *NF2* alterations. Similarly, increased expression of EZH2, but not MYC, was shown to be associated with the most aggressive phenotype in combination with *NF2* alterations. E2F1 is known to promote malignant behaviors in various cancers, including cell proliferation and metastasis. To our knowledge, there is no commercially available drug directly targeting E2F1.

Expression of EZH2, the enzymatic component of the Polycomb Repressive Complex 2 (PRC2), was also reported to be associated with a higher histological grade and worse patient prognosis in meningiomas [10, 26, 39]. Aggressive meningiomas are characterized by genome-wide DNA hypermethylation [10], and the upregulation of *EZH2* concomitant with hypermethylation of PRC2 target sites has been reported in atypical meningiomas or those that have undergone malignant transformation [10, 26]. *EZH2* is one of the direct targets of E2F1 and may additionally be upregulated via Yes1 Associated Transcriptional Regulator (YAP)/transcriptional coactivator with PDZ-binding motif (TAZ) activation by loss of Merlin in meningiomas [8, 16]. Importantly, the present study demonstrated that upregulation of *EZH2* in combination with *NF2* alterations underlies the molecular characteristics of the most aggressive meningiomas. Although complete tumor regression was not observed, our in vitro analyses demonstrated that tazemetostat suppressed the growth of multiple meningioma cell lines with unknown *NF2* status in a manner that appeared to depend on the level of EZH2 expression. Since YAP has also been shown to cooperate with both E2F1 and EZH2 in the regulation of many cell-cycle-related genes [16], combining an EZH2 inhibitor with either a NF2 or YAP inhibitor might be an attractive therapeutic strategy for aggressive meningiomas.

Moreover, EZH2 is known to orchestrate tumor immune evasion via H3K27me3 by transcriptionally silencing the Major Histocompatibility Complex (MHC) class I-dependent antigen presentation pathway [4, 33] and repressing the production of T-cell-recruiting chemokines such as CXCL9 and CXCL10 [22, 27]. Indeed, previous studies reported that the expression of EZH2 was correlated with PD-L1 expression and an immunosuppressive tumor microenvironment in cancers including meningioma [35, 39]. Therefore, the upregulation of EZH2 might be associated with downregulation of immune/inflammatory response in aggressive meningiomas, suggesting the potential efficacy of immunotherapy combined with an EZH2 inhibitor [11, 15]. ARID1A is a subunit of the Switch/Sucrose Non-Fermentable (SWI/SNF) chromatin remodeling complex and has been shown to play a role in tumor suppression. Mutations in *ARID1A* are found in approximately 6% of human cancers and have attracted attention as therapeutic targets leveraging synthetic lethality [40]. A previous study reported that mutations in *ARID1A* were found in 12 of 88 (13.6%) atypical meningiomas [5]; however, in the present cohort, mutations in *ARID1A* were not found in any of the cases. Instead, immunohistochemical analysis showed that expression of ARID1A is increased in higher-grade meningiomas compared to grade 1 meningiomas. Because ARID1A is known to play a role in maintaining genomic integrity and repairing DNA damage [18], its increased expression might be a result of the increased genomic instability of higher-grade tumors. The present

study has some limitations. The number of cases of the discovery cohort was small, and four of the 28 tumors in the cohort were recurrent following radiotherapy, which could have influenced the genomic status of the tumors. However, the results drawn from the analyses of our cohort were validated in previously published larger datasets, suggesting the generalizability and clinical utility of our results. Another limitation is that an in vivo model for MZ857M, a meningioma cell line established from patient surgical tissue, is currently unavailable.

Conclusions

The present study demonstrated that meningiomas might sequentially progress via the downregulation of immune/inflammatory responses, followed by the upregulation of the cell cycle and DNA replication, and that aggressive meningiomas are characterized by upregulation of *EZH2* as well as *E2F1* in combination with *NF2* alterations. These findings, together with our in vitro analyses, suggest that targeting EZH2 alone or in combination with inhibitors of NF2, YAP, or immune checkpoints, shows potential efficacy for high-grade meningiomas.

Abbreviations

AKT1: AKT Serine/Threonine Kinase 1:

ARID1A: AT-rich interaction domain 1A:

CDKN2A: Cyclin-Dependent Kinase Inhibitor 2A:

CNA: chromosomal number aberration:

DEG: differentially expressed gene:

E2F: E2F Transcription Factor

EZH2: enhancer of zeste homolog 2:

FDR: false discovery rate

FOXM1: Forkhead Box M1 gene

GSEA: gene set enrichment analysis

GSVA: gene set variation analysis

H3K27me3: trimethylation of histone 3 lysine 27

IL6: Interleukin 6

JAK: Janus kinase

KLF4: KLF Transcription Factor 4

MHC: Major Histocompatibility Complex

MYC: MYC Proto-Oncogene

NGS: next generation sequencing

NF2: Moesin-Ezrin-Radixin Like (MERLIN) Tumor Suppressor

PDGFR: platelet drived frowth factor receptor

SMO: Smoothened, Frizzled Class Receptor

SSTR2A: somatostatin receptor subtype 2A

STAT3: Signal Transducer and Activator of Transcription 3

SWI/SNF: Switch/Sucrose Non-Fermentable

TAZ: transcriptional coactivator with PDZ-binding motif

TERT: Telomerase Reverse Transcriptase

TRF7: TNF Receptor Associated Factor 7

YAP: Yes1 Associated Transcriptional Regulator

Declarations

Ethics approval and consent to participate

The study was compliant with the ethical guidelines for Medical and Health Research involving Human Subjects in Japan, and was approved by the Ethics Committee at Keio University School of Medicine (20050002). All patients provided written informed consent.

Consent for publication

The patients signed informed consent forms for the use of surgical material and anonymized health information for scientific purposes and publication. All authors have approved the publication of the study.

Funding

The present work was supported by a Grant-in-Aid for Scientific Research (KAKENHI) from the Ministry of Education, Culture, Sports, Science and Technology (Grant no. 19K09464).

Author Contribution

RS and H Sasaki contributed to the acquisition of tumor samples and developed the study concept and design. All authors contributed to data analysis and interpretation of the results; TT and H Saya performed hierarchical clustering, GSEA, and GSVA; KN, EA and HN contributed to NGS and immunohistochemistry; and KY and SY performed cell culture experiments. RS, TT, KN, KY, SO, and H Sasaki wrote the original draft.

Acknowledgement

We thank Prof. Masahiro Toda of the Department of Neurosurgery, Keio University School of Medicine, Japan, and Prof. Yoshiko Okita of the Department of Neurosurgery, Faculty of Medicine, Miyazaki University, Japan, for their guidance and supervision. We also thank Dr. Kensuke Tateishi at the Department of Neurosurgery, Yokohama City University School of Medicine, Japan for helpful discussion.

Data Availability

The data presented in the current study are available within the article and Supplementary files or from the corresponding author upon reasonable request.

References

1. Blighe KRS, Lewis M (2024) EnhancedVolcano: Publication-ready volcano plots with enhanced colouring and labeling. R package version 1.24.0. https://github.com/kevinblighe/EnhancedVolcano
2. Board WCTE (2021) Central nervous system tumours. WHO classification of tumours series. International Agency for Research on Cancer, City
3. Brastianos PK, Twohy EL, Gerstner ER, Kaufmann TJ, Iafrate AJ, Lennerz J, Jeyapalan S, Piccioni DE, Monga V, Fadul CE al (2023) Alliance A071401: Phase II Trial of Focal Adhesion Kinase Inhibition in Meningiomas With Somatic NF2 Mutations. J Clin oncology: official J Am Soc Clin Oncol 41:618–628. 10.1200/jco.21.02371
4. Burr ML, Sparbier CE, Chan KL, Chan YC, Kersbergen A, Lam EYN, Azidis-Yates E, Vassiliadis D, Bell CC, Gilan Oet al et al (2019) An Evolutionarily Conserved Function of Polycomb Silences the MHC Class I Antigen Presentation Pathway and Enables Immune Evasion in Cancer. Cancer Cell 36:385–401e388. 10.1016/j.ccell.2019.08.008
5. Chaluts D, Dullea JT, Ali M, Vasan V, Devarajan A, Rutland JW, Gill CM, Ellis E, Kinoshita Y, McBride RB al (2023) ARID1A mutation associated with recurrence and shorter progression-free survival in atypical meningiomas. J Cancer Res Clin Oncol 149:5165–5172. 10.1007/s00432-022-04442-y

6. Choudhury A, Magill ST, Eaton CD, Prager BC, Chen WC, Cady MA, Seo K, Lucas CG, Casey-Clyde TJ, Vasudevan HN al (2022) Meningioma DNA methylation groups identify biological drivers and therapeutic vulnerabilities. Nat Genet 54:649–659. 10.1038/s41588-022-01061-8
7. Goutagny S, Yang HW, Zucman-Rossi J, Chan J, Dreyfuss JM, Park PJ, Black PM, Giovannini M, Carroll RS, Kalamarides M (2010) Genomic profiling reveals alternative genetic pathways of meningioma malignant progression dependent on the underlying NF2 status. Clin cancer research: official J Am Association Cancer Res 16:4155–4164. 10.1158/1078 – 0432.Ccr-10-0891
8. Guo P (2026) Merlin-YAP signaling: emerging mechanisms, functions, and therapeutic approaches. Trends Cell Biol 36:301–311. 10.1016/j.tcb.2025.09.001
9. Hänzelmann S, Castelo R, Guinney J (2013) GSVA: gene set variation analysis for microarray and RNA-seq data. BMC Bioinformatics 14:7. 10.1186/1471-2105-14-7
10. Harmancı AS, Youngblood MW, Clark VE, Coşkun S, Henegariu O, Duran D, Erson-Omay EZ, Kaulen LD, Lee TI, Abraham BJ et al (2017) Integrated genomic analyses of de novo pathways underlying atypical meningiomas. Nat Commun 8: 14433 10.1038/ncomms14433
11. Jeong Y, Jang H, Kim SB, Yu M, Kim RE, Choi WS, Jeon Y, Lim JY (2025) Dual targeting of EZH2 and PD-L1 in Burkitt's lymphoma enhances immune activation and induces apoptotic pathway. Front Immunol 16:1578665. 10.3389/fimmu.2025.1578665
12. Korotkevich GSV, Sergushichev A (2019) Fast gene set enrichment analysis. http://biorxiv.org/content/early/2016/06/20/060012
13. Liberzon A, Birger C, Thorvaldsdóttir H, Ghandi M, Mesirov JP, Tamayo P (2015) The Molecular Signatures Database (MSigDB) hallmark gene set collection. Cell Syst 1:417–425. 10.1016/j.cels.2015.12.004
14. Liberzon A, Subramanian A, Pinchback R, Thorvaldsdóttir H, Tamayo P, Mesirov JP (2011) Molecular signatures database (MSigDB) 3.0. Bioinformatics 27:1739–1740. 10.1093/bioinformatics/btr260
15. Lin Q, Wu F, Zhang L, Zhang Y, Sun S, Wu X, Yu H (2026) EZH2 inhibition overcomes immune evasion in lung adenocarcinoma by restoring CCL5-mediated T-cell recruitment and MHC class I antigen presentation. Acta Biochim Biophys Sin (Shanghai). 10.3724/abbs.2026013
16. Lo Sardo F, Pulito C, Sacconi A, Korita E, Sudol M, Strano S, Blandino G (2021) YAP/TAZ and EZH2 synergize to impair tumor suppressor activity of TGFBR2 in non-small cell lung cancer. Cancer Lett 500:51–63. 10.1016/j.canlet.2020.11.037
17. Louis DN, Ohgaki H, Wiestler OD, Cavenee WK, Ellison DW, Figarella-Branger D, Perry A, Reifenberger G, von Deimling A (2016) WHO classification of tumours of the central nervous system. International agency for research on cancer, City
18. Mandal J, Mandal P, Wang TL, Shih IM (2022) Treating ARID1A mutated cancers by harnessing synthetic lethality and DNA damage response. J Biomed Sci 29:71. 10.1186/s12929-022-00856-5
19. Mawrin C, Perry A (2010) Pathological classification and molecular genetics of meningiomas. J Neurooncol 99:379–391. 10.1007/s11060-010-0342-2

20. McCarty KS Jr., Miller LS, Cox EB, Konrath J, McCarty KS, Sr (1985) Estrogen receptor analyses. Correlation of biochemical and immunohistochemical methods using monoclonal antireceptor antibodies. Arch Pathol Lab Med 109:716–721
21. Mootha VK, Lindgren CM, Eriksson KF, Subramanian A, Sihag S, Lehar J, Puigserver P, Carlsson E, Ridderstråle M, Laurila E al (2003) PGC-1alpha-responsive genes involved in oxidative phosphorylation are coordinately downregulated in human diabetes. Nat Genet 34:267–273. 10.1038/ng1180
22. Nagarsheth N, Peng D, Kryczek I, Wu K, Li W, Zhao E, Zhao L, Wei S, Frankel T, Vatan L al (2016) PRC2 Epigenetically Silences Th1-Type Chemokines to Suppress Effector T-Cell Trafficking in Colon Cancer. Cancer Res 76:275–282. 10.1158/0008-5472.Can-15-1938
23. Nakamura K, Aimono E, Oba J, Hayashi H, Tanishima S, Hayashida T, Chiyoda T, Kosaka T, Hishida T, Kawakubo Het al et al (2021) Estimating copy number using next-generation sequencing to determine ERBB2 amplification status. Med Oncol 38:36. 10.1007/s12032-021-01482-1
24. Nassiri F, Liu J, Patil V, Mamatjan Y, Wang JZ, Hugh-White R, Macklin AM, Khan S, Singh O, Karimi Set al et al (2021) A clinically applicable integrative molecular classification of meningiomas. Nature 597:119–125. 10.1038/s41586-021-03850-3
25. Nukaya T, Sumitomo M, Sugihara E, Takeda M, Nohara S, Tanishima S, Takenaka M, Zennami K, Takahara K, Shiroki R, Saya H (2023) Estimating copy number to determine BRCA2 deletion status and to expect prognosis in localized prostate cancer. Cancer Med 12:8154–8165. 10.1002/cam4.5617
26. Ohara K, Miyawaki S, Teranishi Y, Komura D, Okano A, Hongo H, Dofuku S, Ishigami D, Sakai Y, Shimada D et al (2025) Sequential omics analysis reveals molecular signatures of malignant transformation in recurrent meningiomas. Acta neuropathologica communications 13: 235 10.1186/s40478-025-02149-y
27. Peng D, Kryczek I, Nagarsheth N, Zhao L, Wei S, Wang W, Sun Y, Zhao E, Vatan L, Szeliga Wet al et al (2015) Epigenetic silencing of TH1-type chemokines shapes tumour immunity and immunotherapy. Nature 527:249–253. 10.1038/nature15520
28. Sahm F, Aldape KD, Brastianos PK, Brat DJ, Dahiya S, von Deimling A, Giannini C, Gilbert MR, Louis DN Raleigh DR (2025) cIMPACT-NOW update 8: Clarifications on molecular risk parameters and recommendations for WHO grading of meningiomas. Neurooncology 27: 319–330 10.1093/neuonc/noae170
29. Sahm F, Schrimpf D, Stichel D, Jones DTW, Hielscher T, Schefzyk S, Okonechnikov K, Koelsche C, Reuss DE, Capper D et al (2017) DNA methylation-based classification and grading system for meningioma: a multicentre, retrospective analysis. The lancet oncology 18: 682–694 10.1016/s1470-2045(17)30155-9
30. Sasaki H (2023) [Meningioma]. No Shinkei Geka 51:829–836 Doi 10.11477/mf.1436204824
31. Shih KC, Chowdhary S, Rosenblatt P, Weir AB 3rd, Shepard GC, Williams JT, Shastry M, Burris HA 3rd, Hainsworth JD (2016) A phase II trial of bevacizumab and everolimus as treatment for patients with

refractory, progressive intracranial meningioma. J Neurooncol 129:281–288. 10.1007/s11060-016-2172-3

32. Subramanian A, Tamayo P, Mootha VK, Mukherjee S, Ebert BL, Gillette MA, Paulovich A, Pomeroy SL, Golub TR, Lander ES, Mesirov JP (2005) Gene set enrichment analysis: a knowledge-based approach for interpreting genome-wide expression profiles. Proc Natl Acad Sci U S A 102:15545–15550. 10.1073/pnas.0506580102
33. Sun S, Yu F, Xu D, Zheng H, Li M (2022) EZH2, a prominent orchestrator of genetic and epigenetic regulation of solid tumor microenvironment and immunotherapy. Biochim Biophys Acta Rev Cancer 1877:188700. 10.1016/j.bbcan.2022.188700
34. Team C (2023) R: A Language and Environment for Statistical Computing. RFoundation for Statistical Computing. https://www.R-project.org/
35. Toyokawa G, Takada K, Tagawa T, Hamamoto R, Yamada Y, Shimokawa M, Oda Y, Maehara Y (2019) A Positive Correlation Between the EZH2 and PD-L1 Expression in Resected Lung Adenocarcinomas. Ann Thorac Surg 107:393–400. 10.1016/j.athoracsur.2018.08.056
36. Wang JZ, Landry AP, Raleigh DR, Sahm F, Walsh KM, Goldbrunner R, Yefet LS, Tonn JC, Gui C, Ostrom QT al (2024) Meningioma: International Consortium on Meningiomas consensus review on scientific advances and treatment paradigms for clinicians, researchers, and patients. Neurooncology 26:1742–1780. 10.1093/neuonc/noae082
37. Yokogami K, Kikuchi T, Watanabe T, Nakatake Y, Yamashita S, Mizuguchi A, Takeshima H (2022) Methionine regulates self-renewal, pluripotency, and cell death of GIC through cholesterol-rRNA axis. BMC Cancer 22:1351. 10.1186/s12885-022-10280-5
38. Yokogami K, Watanabe T, Yamashita S, Mizuguchi A, Takeshima H (2024) Inhibition of BMP signaling pathway induced senescence and calcification in anaplastic meningioma. J Neurooncol 167:455–465. 10.1007/s11060-024-04625-2
39. Zeng J, Sun L, Huang J, Yang X, Hu W (2022) Enhancer of zeste homolog 2 is a negative prognostic biomarker and correlated with immune infiltrates in meningioma. Front Neurosci 16:1076530. 10.3389/fnins.2022.1076530
40. Zhang X, Zhang Y, Zhao J, Wu Y, Zhang N, Shen W (2023) ARID1A mutations in cancer development: mechanism and therapy. Carcinogenesis 44:197–208. 10.1093/carcin/bgad011

Figures

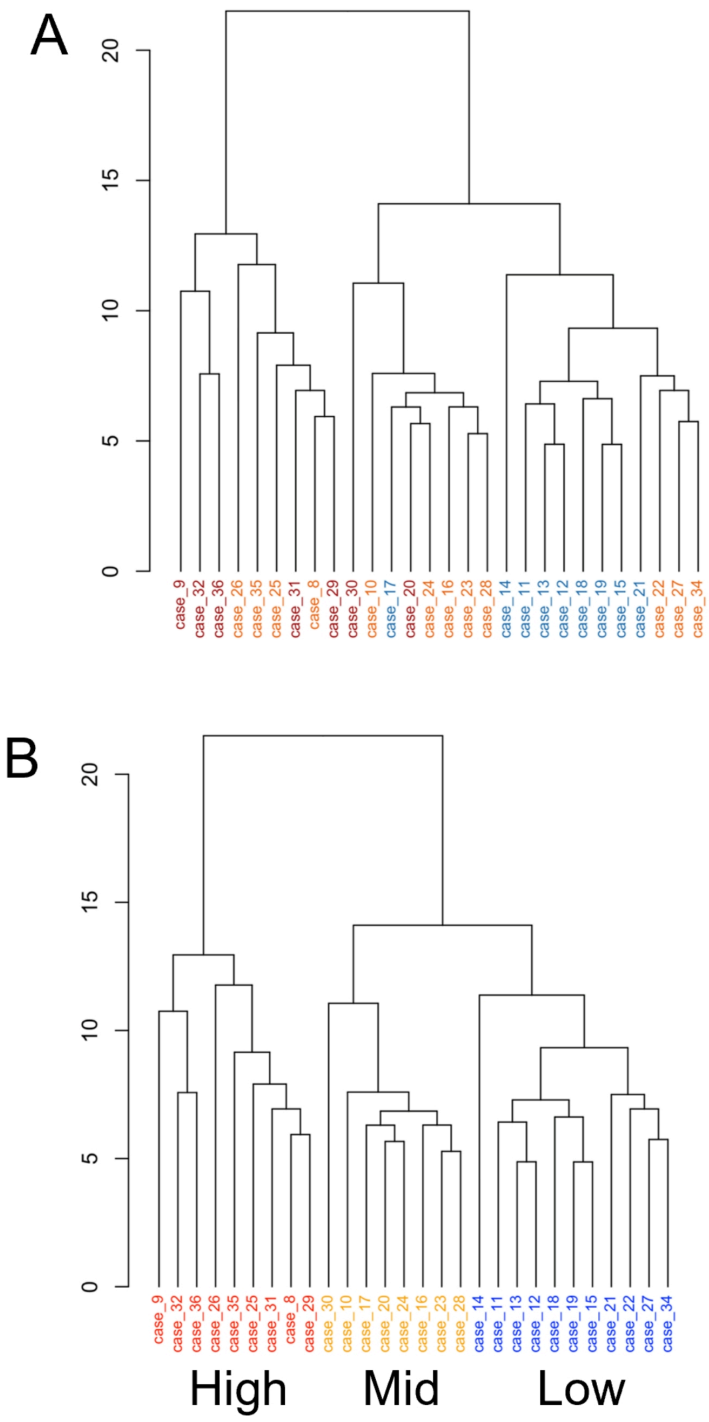


Figure 1

A, Unsupervised clustering of 28 meningiomas based on the expression of differentially expressed genes across tumor histological grades. Blue, orange, and red letters indicate grade 1, 2, and 3 tumors, respectively. The 28 tumors were classified into 3 groups, and the composition of each group appeared to be correlated with tumor histological grade. B, The resulting 3 groups were named as Low, Mid, and High, and this grouping was defined as Cluster M.

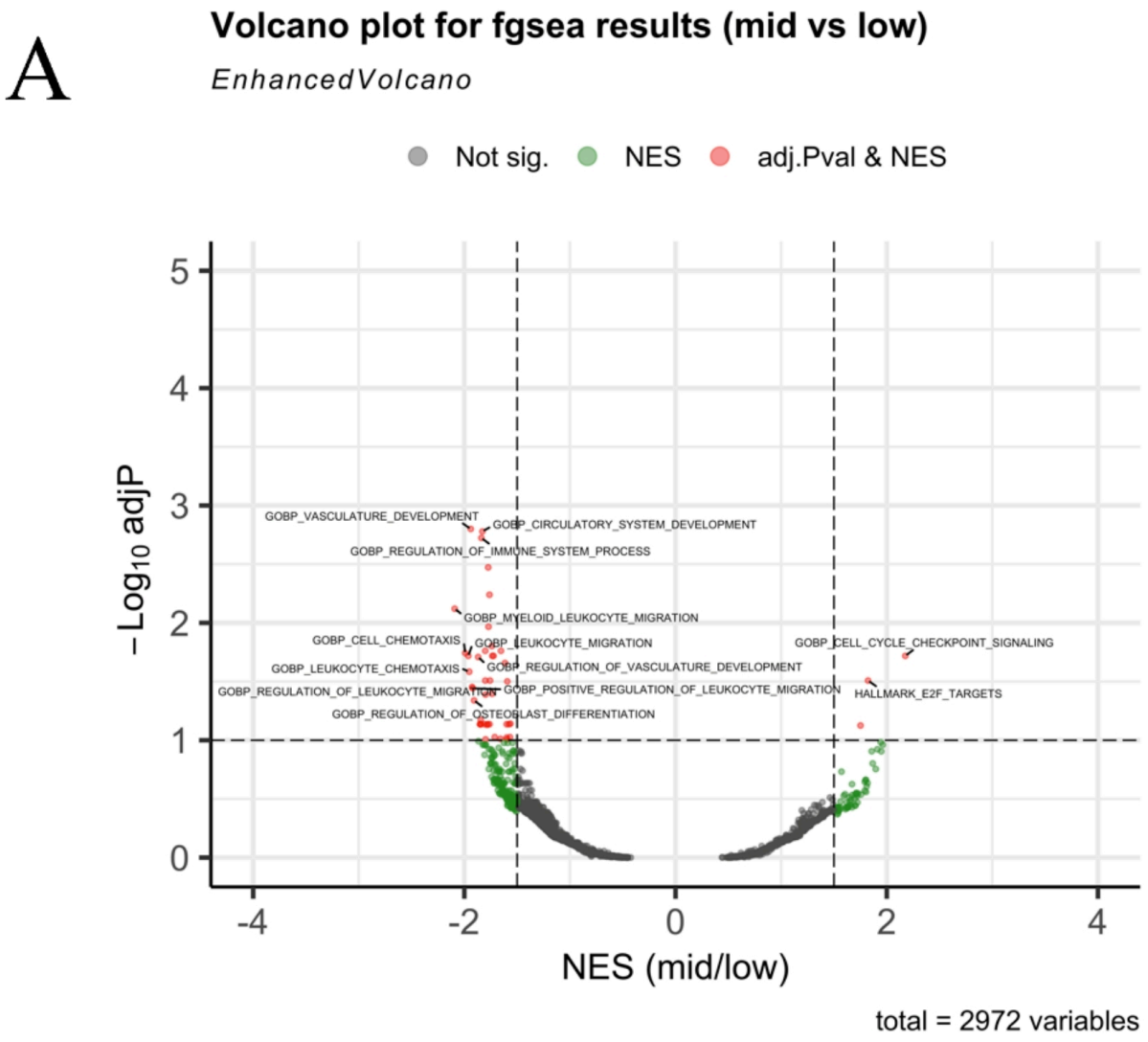


Figure 2

A, Volcano plot for GSEA results between the Mid and Low groups of Cluster M. B, Volcano plot for GSEA results between the High and Midgroups of Cluster M.

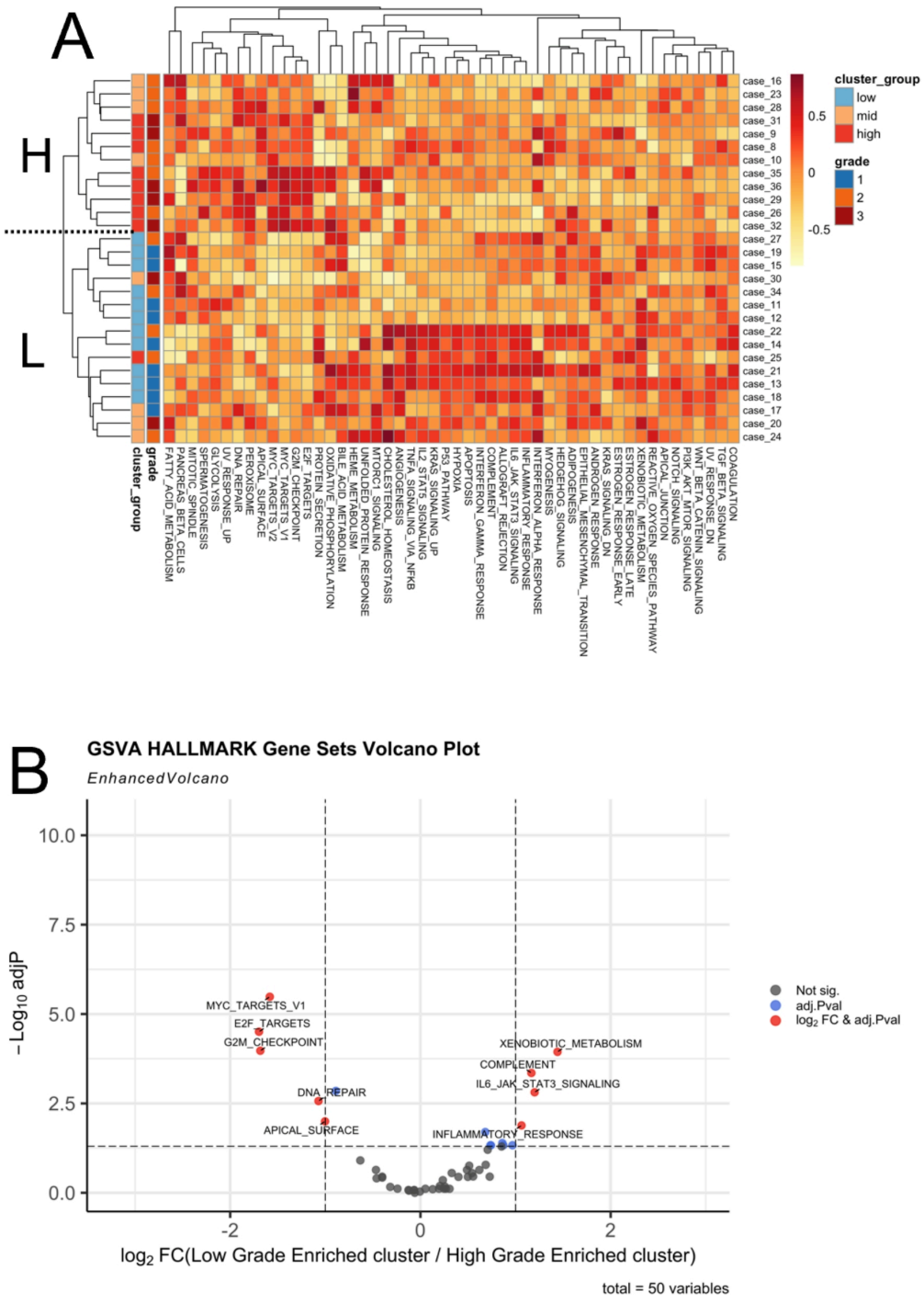


Figure 3

A, Hierarchical clustering based on the enrichment score for the Hallmark gene sets. The clustering divided the cases into two clusters (H and L separated by the dotted line), which correlated with Cluster M as well as tumor histological grade. B, Volcano plot for Hallmark gene sets based on FDR and fold change between the two clusters. Note that gene sets associated with oncogene targets and the cell

cycle are upregulated, and gene sets associated with the immune/inflammatory response and biological defense are downregulated in H compared to L.

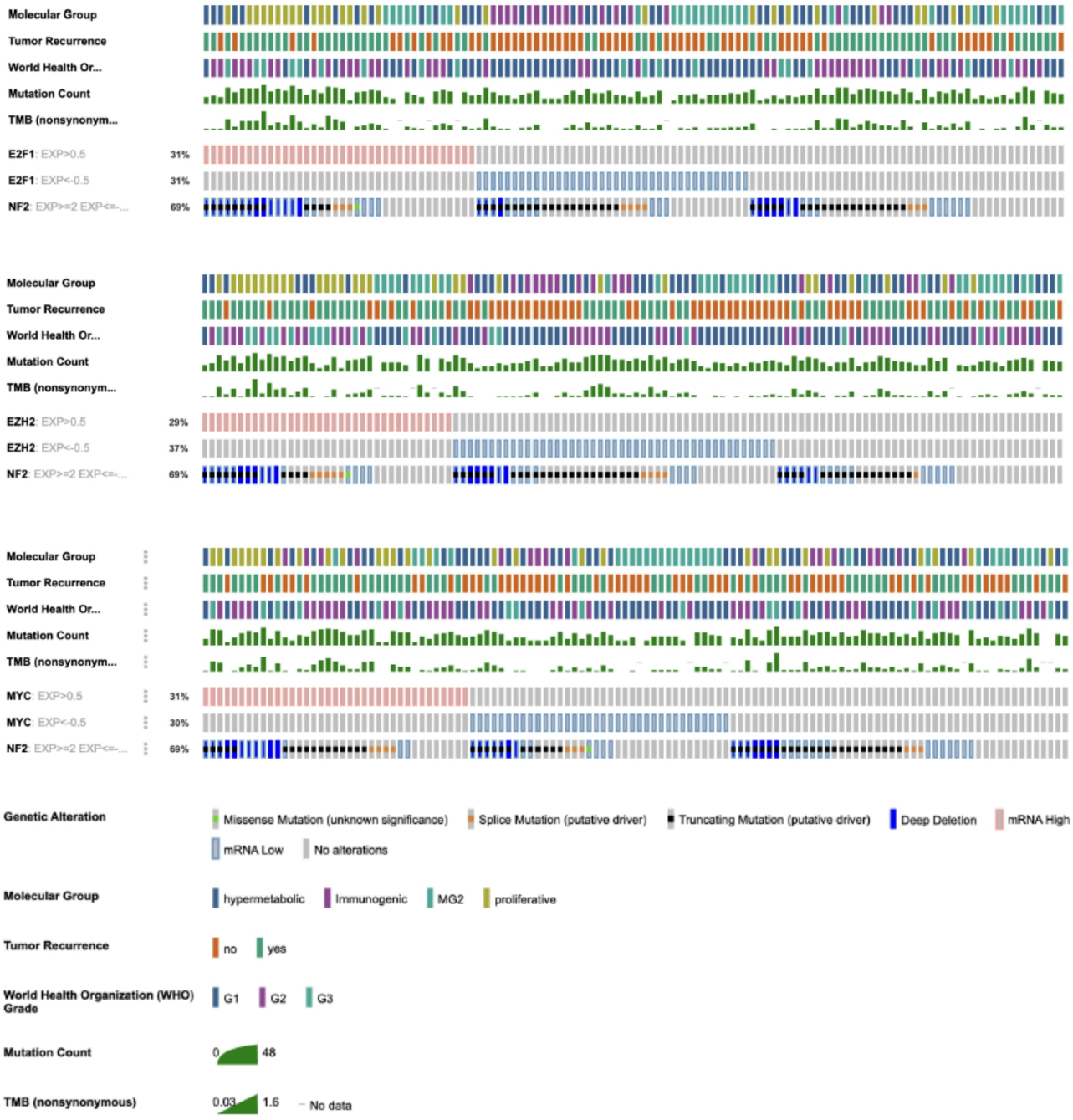


Figure 4

OncoPrint analyses of the expression of E2F1 (top), EZH2 (middle), MYC (bottom), and NF2 genetic alterations based on the published dataset (Nassiri et al.). Note that tumors with high E2F1 expression in combination with NF2 alterations were mostly MG4 (proliferative) tumors, while no MG1 (immunogenic)

tumors exhibited these characteristics (high E2F1 expression and NF2 alterations). Moreover, most of the MG1 tumors were associated with low E2F1 expression. Similarly, the tumors with high EZH2 expression in combination with NF2 alterations were mostly MG4, while most of the MG1 tumors were associated with low EZH2 expression. On the other hand, in the MYC OncoPrint, the tendency was less pronounced; MG1 tumors were dispersed regardless of the expression of MYC, and some of the tumors with high MYC expression in combination with NF2 alterations were MG1.

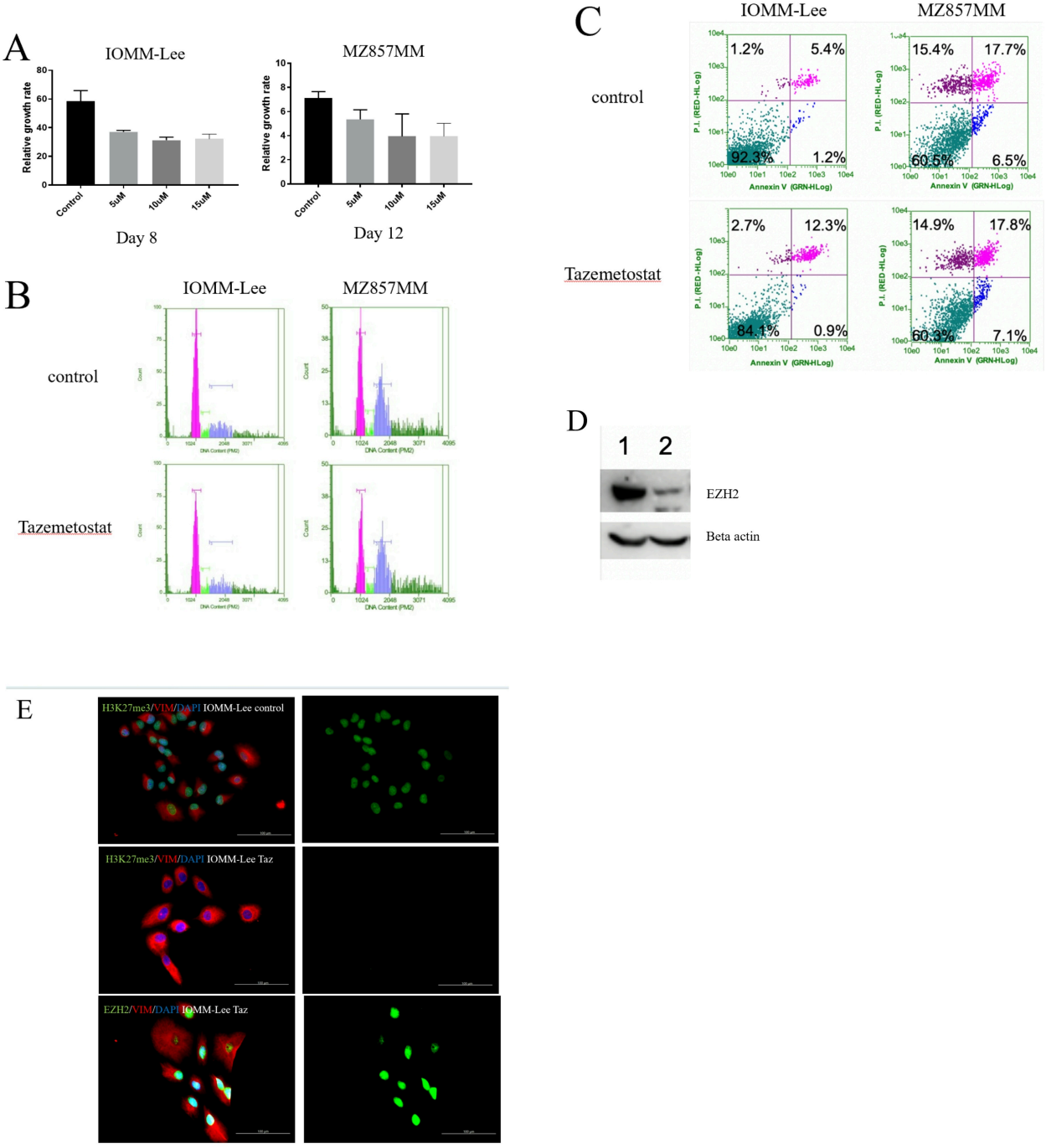


Figure 5

A, WST-8 assay showing the suppression of meningioma cell growth with various concentrations of tazemetostat. Relative growth rate indicates the fold increase in cell number compared to day 1. B, cell cycle assay showing an increase in the sub-G1 population in meningiomas treated with tazemetostat. C, annexin V assay showing an increase in apoptosis in meningiomas treated with tazemetostat, especially in IOMM-Lee. D, Western blotting with EZH2. Lane 1: IOMM-Lee. Lane 2: MZ857MM. E, Immunofluorescence staining of IOMM-Lee cells. Note that tazemetostat decrease H3K27 trimethylation, but not EZH2 levels.

Supplementary Files

This is a list of supplementary files associated with this preprint. Click to download.

- SupplementaryTables.docx
- SupplemetaryFigures.pptx